Jour. of the KGS, Vol. 20, No. 7. September 2004, pp. 107~117

Bearing Capacity of Shallow Foundation on Geosynthetic Reinforced Sand

토목섬유로 보강된 얕은기초 모래지반의 지지력

Won, Myoung-Soo[1] 원 명 수
Ling, Hoe I.[2] 링 호
Kim, You-Seong[3] 김 유 성

요 지

느슨한 모래지반에서 보강재 층수 증가와 보강재의 강성과 형태 변화 그리고 얕은 기초 직하에 매설된 연성관의 깊이 등의 변화가 지지력-침하 곡선에 미치는 영향을 알아보기 위해 일련의 모형실험을 수행하였다. 시험결과, 무보강토 경우는 파괴형태가 국부전단으로 나타났으나 보강재 층수가 2층 이상이 되면 파괴형태는 국부전단에서 전반전단으로 바뀌고, 최적보강재 층수는 2층 이며, 지지력 개선에 있어서는 보강재의 초기강성과 형태가 최대인장강도보다 중요한 것으로 나타났다. 무보강토에서 기초 직하에 연성관이 매설된 경우, 연성관의 매설 깊이가 기초 폭보다 얕으면 지지력과 극한지지력은 현저하게 감소하고, 보강토의 경우 연성관의 매설 깊이가 기초 폭보다 얕으면 파괴형태는 전반전단에서 국부전단으로 바뀌는 것으로 나타났다.

Abstract

A series of model tests were conducted to investigate how the number of reinforcement layers, stiffnesses, types of reinforcement material and buried depth of a flexible pipe can affect bearing capacity-settlement curve at a loose sand foundation. In the test results, whereas the type of failure in unreinforced sand was local shear, the type of failure, for model tests with more than 2 reinforcement layers in loose sand, was general shear: The number of the optimum reinforcement layers was found to be two; Stiffness and type of reinforcement were more important than the maximum tensile strength of reinforcement in improving bearing capacity. When the depth of buried pipe from the sand surface was less than the width of the footing, test results showed that both bearing capacity and ultimate bearing capacity of buried pipe in unreinforced sand significantly decreased, and the type of failure in the reinforced sand changed from general shear to local shear.

Keywords : Bearing capacity, Flexible pipe, Geosynthetic, Reinforced sand, Shallow foundation

1. Introduction

Since Binquet & Lee (1975) reported first the systematic study results on bearing capacity of reinforced soil, numerous analytical and experimental studies on this subject have been performed by several researchers (Akinmusuru & Akinbolade, 1981; Guido et al., 1986, 1987; Sridharan et al., 1989; Samtani & Sonpal, 1989;

1 Member, Manager, Research Institute of Technology, KSM Engrg. CO., LTD., Korea (wondain@kunsan.ac.kr)
2 Asst. Prof., Dept. of Civil Engrg., Columbia Univ., New York, NY
3 Member, Asst. Prof., Dept. of Civil Engrg., Chonbuk National Univ., Korea

Huang & Tatsuoka, 1988, 1990; Abled-Baki et al., 1993; Khing et al., 1993; Omar et al., 1993a, b; and Yetimoglu et al., 1994). According to their reported results, bearing capacity was improved remarkably when tensile reinforcements, such as metal bars or geo-synthetics, were placed horizontally beneath footing.

The main parameters involved in this study are the distance of the first reinforcement level from the bottom of the footing (u), the vertical spacing of reinforcement layers (h), the length of the reinforcement (b), and the number of reinforcement layers (N) as included in Fig. 10.

It has been reported that the optimum depth of the first reinforcement layer is between 0.25B and 0.5B (Akinmusuru & Ankubolance, 1981; Guido et al., 1987; Shin et al., 1999; Yetimoglu et al., 1994) beneath the footing; the optimum vertical spacing of the reinforcement layer is between 0.15B and 0.4B (Singh, 1988; Yetimoglu et al., 1994); the optimum reinforcement length is 6B~8B (Fragaszy & Lawton, 1984; Huang & Tatsuoka, 1988; Mandal & Manjunath, 1990; Khing et al., 1993; Omar et al., 1993), and the optimum number of reinforcement layers is 3~6 (Binquet & Lee, 1975a; Guido et al., 1986, 1987; Khing et al., 1993; Yetimoglu et al., 1994).

There are two failure mechanisms for reinforced ground loaded with a footing; one is the anchoring mechanism proposed by Binquet & Lee (1975) and the other is the strain-restraining mechanism proposed by Huang & Tatsuoka (1988).

Of the anchoring mechanism, reports indicate that reinforcement length should be sufficiently longer than the width of footing in order to resist the downwards displacement of the zone immediately beneath the footing. Of the strain-restraining mechanism, prevision literatures indicate that the reinforcement layers with length similar to the width of the footing can remarkably increase the bearing capacity as compressive strength of the reinforced zone increases.

Through a series of model tests, this study intends to investigate how the depth of the buried pipe, the number of reinforcement layers, and types of reinforcement material can affect bearing capacity of reinforced ground.

2. Bearing Capacity Ratio

Fig. 1 shows the bearing capacity(load)-settlement curves of the foundation. Deformation at small bearing capacity is elastic, and the q-s curve is almost a straight line (OE section). When passing point E, the active zone between soil particles increases and local shear failure occurs. As the active zone expands, settlement increases. Foundation failure may occur at point F as only a slight increase of load produces a significant amount of settlement. This is called general shear, and corresponding bearing capacity at this point is called ultimate bearing capacity. This failure mainly takes place in dense sand.

Local shear failure is likely to occur in medium dense sand and its bearing capacity-settlement curve is characterized by a vaguely definable slip path.

The shape of the bearing capacity-settlement curve varies in accordance with the soil's compressibility and shear character, the setting condition of the foundation, and loading method, etc. Fig. 1 (b) shows the force resisting the load, compression resistance, and passive pressure acting at section I when section II is expanding horizontally. For such resistances to take place, several types of bearing-capacity curves can occur under the above condition.

Fig. 2 indicates types of failure that occur with varying relative density, relative depths, d/B, and the shape of foundation.

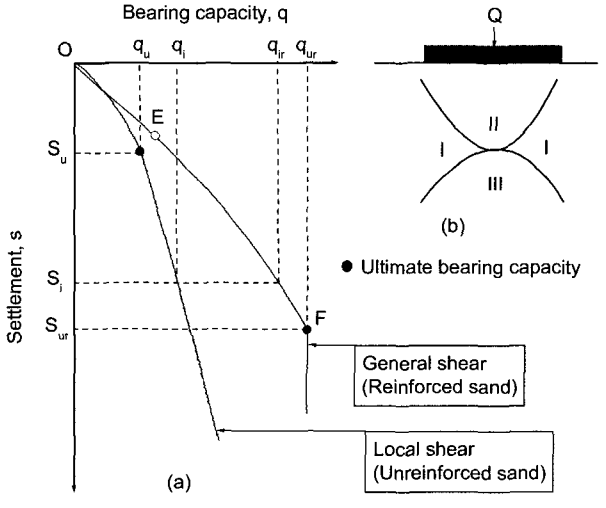

Fig. 1. Bearing capacity-settlement curve

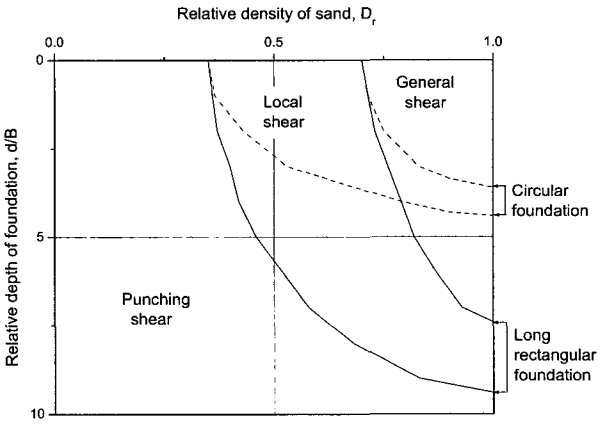

Fig. 2. Variation of the nature of bearing capacity failure in sand with relative density D_r and relative depth d/B (Vesic, 1963)

With large relative depth, local shear or punching shear easily occurs in dense sand because shear behavior is limited to the bottom of the foundation. Circular foundations, compared to rectangular foundations, have the tendency to produce local shear failure due to localized activity because sand around the circular foundation spreads out more easily.

To compare bearing capacity-settlement behavior of reinforced and unreinforced sand, Binquet & Lee (1975a) used a bearing capacity ratio (BCR) defined as follows:

$$BCR_u = q_{ur} / q_u \quad (1)$$

where BCR_u = ultimate bearing capacity ratio,

q_{ur} = ultimate bearing capacity with reinforcement,

q_u = ultimate bearing capacity without reinforcement.

Although q_{ur} is much greater than q_u and reaches the ultimate bearing capacity, the foundation settlement s_{ur} at ultimate bearing capacity (UBC) with reinforced sand is quite a bit larger than the foundation settlement s_u at UBC with unreinforced sand. In practice, foundation settlement is limited in design. Khing et al. (1993) analyzed the reinforcement effect utilizing the same method used by Bingquet & Lee, defining the ratio of BCR as the BCR at a certain settlement level and comparing it with BCR_u :

$$BCR = q_{ir} / q_i \quad (2)$$

where q_{ir} = bearing capacity at a settlement level on reinforced sand,

q_i = bearing capacity at the same settlement level that is reinforced sand on unreinforced sand.

Khing et al. reports that BCR_u is larger than BCR. In these model tests, due to loose sand at a relative density of 50% which leads to local shear failure shown in Figs. 1 and 2, the BCR shown in equation 2 generally was used to analyze the results of the tests.

3. Properties of Testing Materials and Experimental Method

3.1 Properties of Testing Materials

Table 1 and Fig. 3 indicate properties of the sand and the particle size curve; Fig. 4 indicates the relationship

Table 1. Properties of the sand

Property		Value
Dry density (kN/m^3)	Maximum	17.33
	Minimum	13.87
	Used	15.42
Void ratio	Maximum	0.887
	Minimum	0.511
Grain size (mm)	D10	0.107
	D30	0.133
	D60	0.186
Cohesion (kPa)		0
Angle of friction (degrees)		30.86
Specific gravity		2.67
USCS		SP

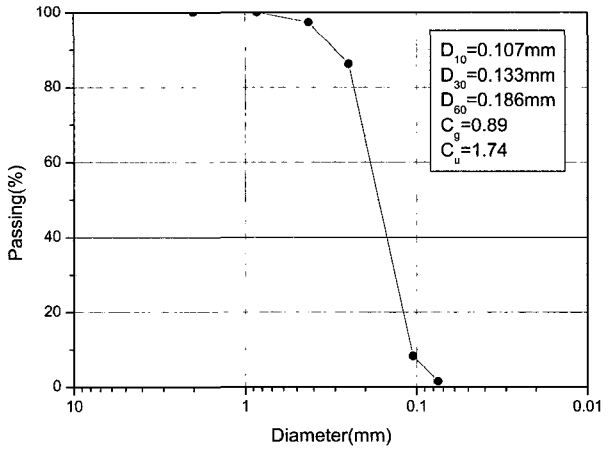

Fig. 3. Particle size distribution curve

between relative density and the falling height. The falling height was approximately 600 mm when the relative density of the sand was 50%. At this point, the unit weight was approximately 1542 kN/m^3. Figs. 5 and 6 show the results of the constant volume shear tests when the sand's relative density was 50% and the cohesion and friction angle of the sand were 0 kPa and 30.86°.

The reinforcements used in this study were metal mosquito mesh and two geogrids which were equal in

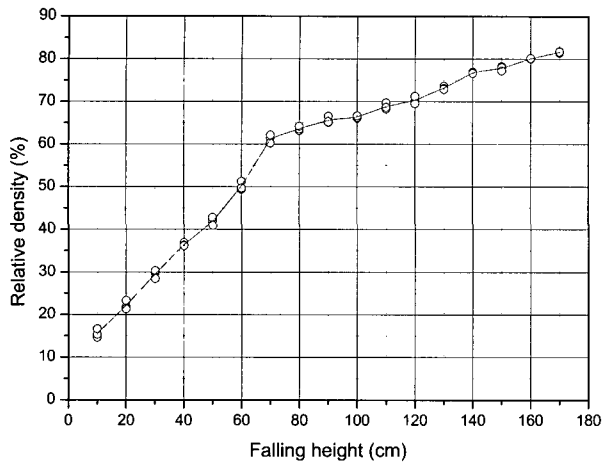

Fig. 4. Relationship between relative density and falling height

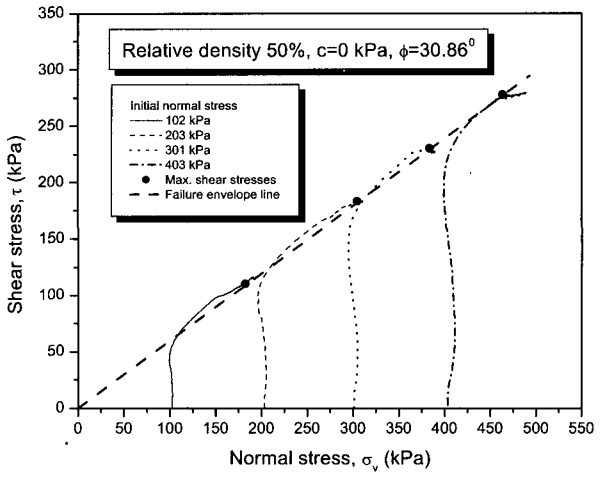

Fig. 6. Results of constant volume shear tests

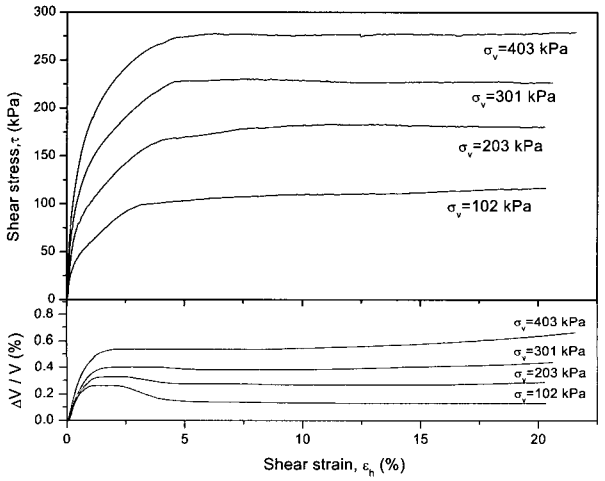

Fig. 5. Shear stress-shear strain curve by a constant volume shear device

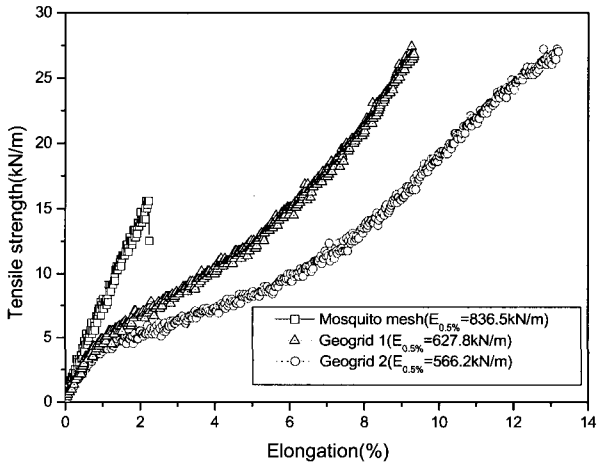

Fig. 7. Tensile strength-elongation properties of the reinforcement

Table 2. Reinforcement properties

	Mosquito mesh	Geogrid 1	Geogrid 2
Rib thickness (mm)	0.4	1.4	0.95
Bar thickness (mm)	0.4	1.4	0.6
Rib width (mm)	0.4	2.3	2
Bar width (mm)	0.4	1.6	5
Aperture length (mm)	1.4	7	20
Aperture width (mm)	1.4	7	20
Tensile strength (ASTM D-4595) (kN/m)	15.6	27.2	27.4
Elongation at yield (ASTM D-4595) (%)	2.2	12.8	9.3
Modulus at 0.5% Elongation (kN/m)	836.5	627.8	566.2

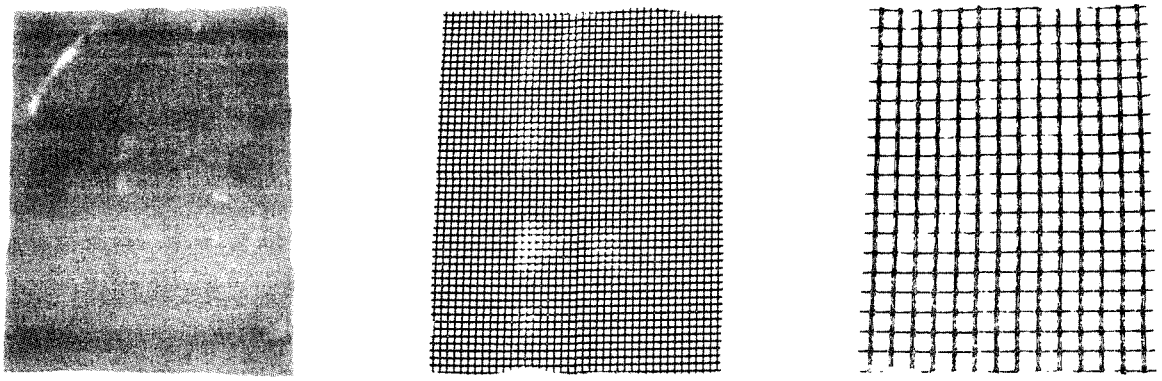

(a) metal mosquito mesh (b) geogrid 1 (c) geogrid 2

Fig. 8. Reinforcement types used in this study

their maximum tensile strength but different in their shapes. Table 2 and Fig. 7 indicate the reinforcement properties and wide-width tensile test results and Fig. 8 shows the reinforcement types.

The flexible pipe used in this study is a PVC pipe, 16.2 mm in its external diameter, 3 mm in its thickness, and 57.96 kPa in its pipe stiffness (ASTM D2413 5%).

3.2 Test Method

Fig. 9 indicates the loading system and placement of samples. The internal dimension of the box in the figure is 880 mm × 450 mm × 980 mm. The walls on both sides perpendicular to the horizontal axis (X) consist of 40 mm thick transparent acrylic plate that allows to observe model behavior. These acrylicic plates are reinforced with 8 steel bars. Each of them 15 mm is thick and 100 mm wide. The walls on both sides are perpendicular to the vertical axis (Y) and consist of 15 mm thick steel plates reinforced in the same manner in order to prevent the deformation of the box during the test. Loading was performed at the speed of 0.5 mm/min.

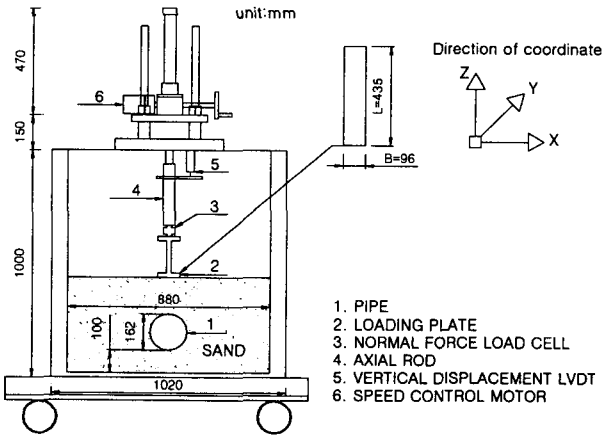

Fig. 9. Schematics of model testing apparatus

It is preferable that the relative density of sandy ground may be higher than 85% to best simulate the actual field condition. However, this test was conducted indoors and there was limitation in the falling height due to the use of rainfall method (see Fig. 4).

Therefore, sand was fallen into the box from the height of 600 mm using the rainfall method, making its relative density 50%. At this point, its void ratio was 0.698.

A flexible pipe, 435 mm in length, is installed 100 mm horizontally above the bottom of the box. In case sand infiltrated into the pipe, the bearing capacity at both ends of the pipe will probably decrease due to collapsing sand that may cause the load to shift and to concentrate at the center of the pipe. To prevent this both ends of the pipe are sealed with sponge which has little compression

Fig. 10. The testing parameter in relation to the reinforcement sand

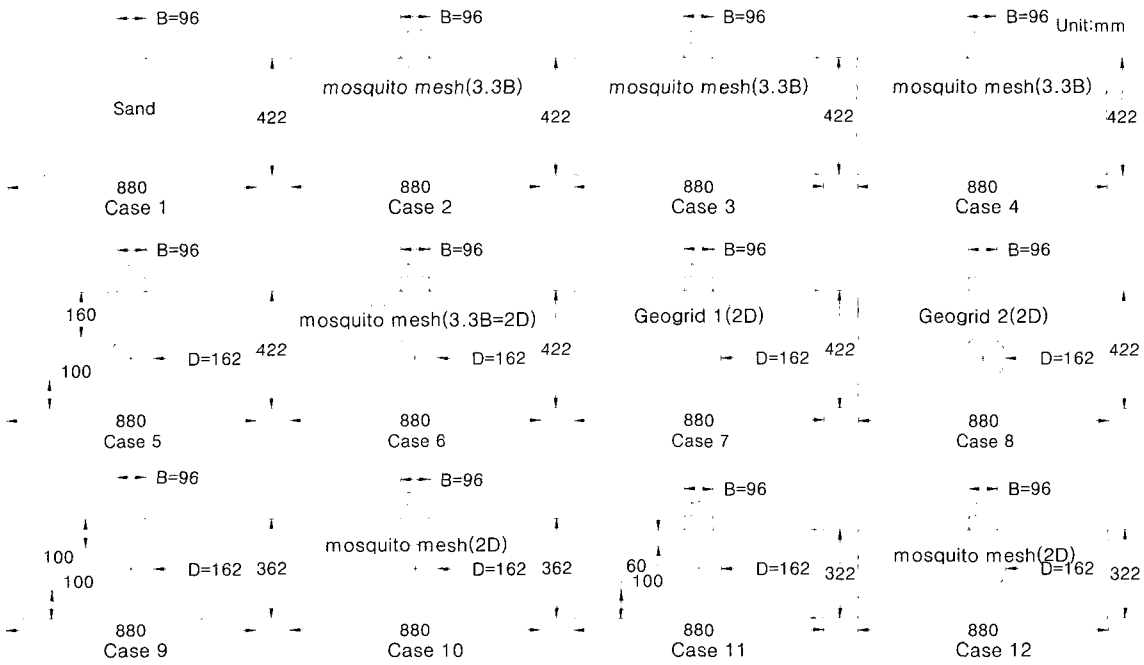

Fig. 11. Sectional view of the model tests

strength and friction with walls.

Fig. 10 indicates the testing parameter in relation to the layout of the reinforcements. The loading plate was 96 mm×435 mm, but the width of the loading plate is assessed at 10mm when reinforcements are installed. The placement of the first reinforcement level is 0.3B (30 mm) from the ground surface, and the vertical spacing of the reinforcement layers is set up at 0.2B (20 mm).

Width of excavation for installing an underground pipe must be set in consideration of the diameter of the pipe. In order to investigate the effects of pipe layout on bearing capacity, the length of the reinforcements is set at 2D=320 mm.

Fig. 11 illustrates a sectional view of the model tests performed in this study. In Fig. 11, Cases 2, 3, 4, 6, 10 and 12 were reinforced with metal mosquito mesh, while Cases 6 and 7 used geogrid as reinforcement. In Cases 5~12, the flexible pipe was buried 100 mm above the bottom of the box.

Cases 1-4 were conducted to determine the optimal number of reinforcement layers by increasing the number of reinforcement layers. Cases 5-8 were conducted to know how different reinforcement materials can affect bearing capacity-settlement curve. Cases 1, 3, 5, 6, & Cases 9-12 study how the buried depth of the pipe and the presence and absence of reinforcements affect bearing capacity-settlement behavior.

4. Analysis of Test Results

4.1 Effect of the Number of Reinforcement Layers

Fig. 12 shows the curve of bearing capacity-settlement behavior with increased reinforcement layers. In the cases of unreinforced sand (Case 1), and only one layer

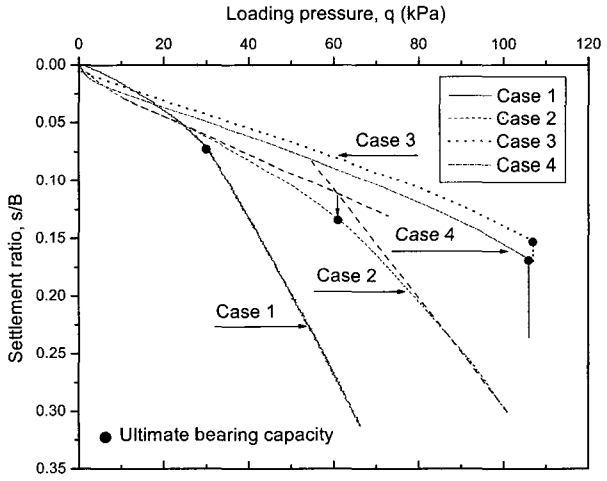

Fig. 12. Bearing capacity-settlement curve in relation to the increase of reinforcement layers

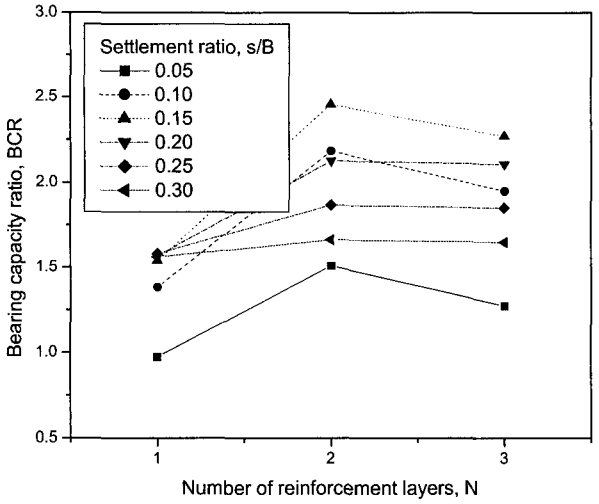

Fig. 13. Bearing capacity ratio in relation to the increase of reinforcement layers

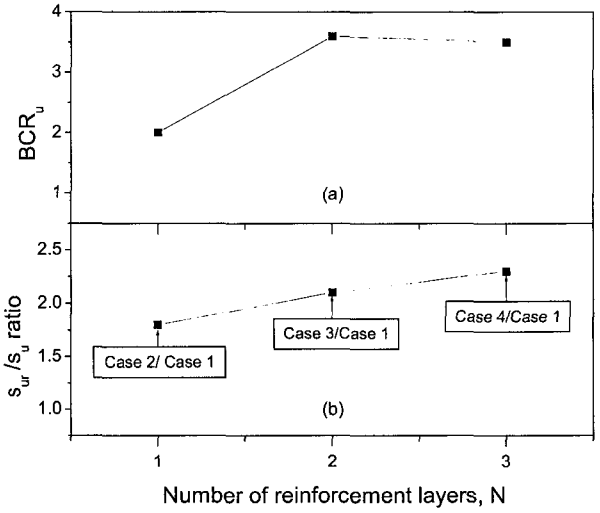

Fig. 14. Ultimate bearing capacity ratio and settlement ratio in relation to the increase of reinforcement layers

of reinforcement (Case 2), the type of failure of the sand is local shear. With more than 2 layers of reinforcement, general shear failure occurred. This figure shows that bearing capacity of the sand significantly improves just by placing the reinforcements. Bearing capacities increased proportionally with the number of reinforcement layers up to 2 layers, but with 3 reinforcement layers, the bearing capacity decreased slightly. We can deduce from this result that the optimal number of reinforcement layers is 2.

When the reinforcement layers increase from 1 to 2, the bearing capacity ratio increases at any settlement ratio. But when the reinforcement layers increase from

Table 3. Ultimate bearing capacity

Case	UBC (kPa)	BCR_{ui}	s_{ui}/B or s_{ur}/B
Case 1	30	1.0	0.0728
Case 2	61	2.0	0.1341
Case 3	107	3.6	0.1531
Case 4	106	3.5	0.1692
Case 5	39	1.3	0.1011
Case 6	107	3.6	0.2141
Case 7	107	3.6	0.2202
Case 8	107	3.6	0.3090
Case 9	28	0.9	0.0787
Case 10	46	1.5	0.1020
Case 11	25	0.8	0.0831
Case 12	38	1.3	0.0892

In which,
UBC = Ultimate bearing capacity
BCR_{ui} = Ultimate bearing capacity ratio = *Case i*/*Case* 1, $i = 2 \sim 12$

2 to 3, the bearing capacity ratio is equal or slightly reduced. At a settlement ratio of 0.15, the bearing capacity ratio is the highest.

Fig. 14 shows the bearing capacity ratio and settlement ratio at the ultimate bearing capacity. The ultimate bearing capacity increases until the number of the reinforcement layers reaches 2, and it remains almost the same when the number of layers is increased from 2 to 3. However, the settlement ratio at the ultimate bearing capacity increases in proportion to the increase of the reinforcement layers.

Table 3 summarizes the ultimate bearing capacity according to each model test and the settlement ratio at the ultimate bearing capacity.

4.2 Effect of Reinforcement Stiffness and Type

Fig. 15 shows quality, stiffness, and shape of reinforcement materials above a flexible pipe buried at a depth of 160 mm from the surface, as seen in Figs. 10 and 11, affect the shape of the bearing capacity-settlement curve. Fig. 16 illustrates the bearing capacity-settlement curve at a given settlement level, in order to examine the reinforcement effect.

The reinforcement used in Case 6 is a metal mosquito mesh that has smaller maximum tensile strength than the

other reinforcement, geogrids. This has high initial stiffness, and the mesh spacing is dense. The reinforcements used in Cases 7 and 8 are geogrids that have similar maximum tensile strength and initial stiffness, but the mesh spacing of reinforcement in Case 7 is more dense than in Case 8 (See Figs. 7 & 10, and Table 2).

As Fig. 15 indicates, general shear occurs if 2 layers of reinforcement materials are used, even with the flexible pipe laid underground; but local shear occurs without reinforcement. Cases 6 and 7 show similar bearing capacity-settlement behaviors while Case 8 shows similar ultimate bearing capacity as in Cases 6 and 7, but shows less bearing capacity at the same settlement level with Cases 6 and 7.

Therefore, to improve bearing capacity, the initial intensity of reinforcements and the mesh spacing appear to be more important factors than the maximum tensile strength of the reinforcement material.

4.3 Effect of Buried Depth of Pipe

Figs. 17 and 18 show the shape of the bearing capacity-settlement curve in relation to various buried depths of pipes with and without reinforcement.

In Case 5, where unreinforced sand is used and flexible pipe is buried at a depth at 1.6B from the foundation, the ultimate bearing capacity is higher than that in Case 1 without the pipe. However, in both cases,

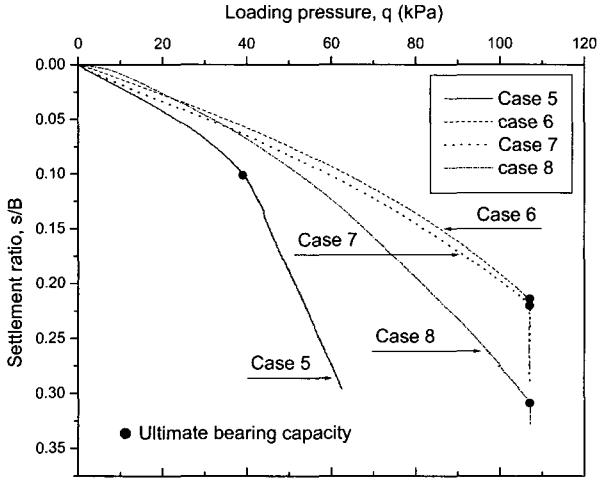

Fig. 15. Bearing capacity-settlement curve in relation to varying stiffnesses and shapes of reinforcement materials

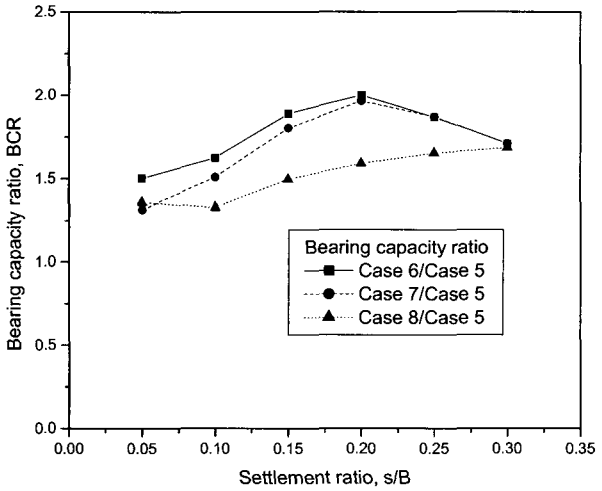

Fig. 16. Bearing capacity ratio in relation to varying stiffnesses and shapes of reinforcement materials

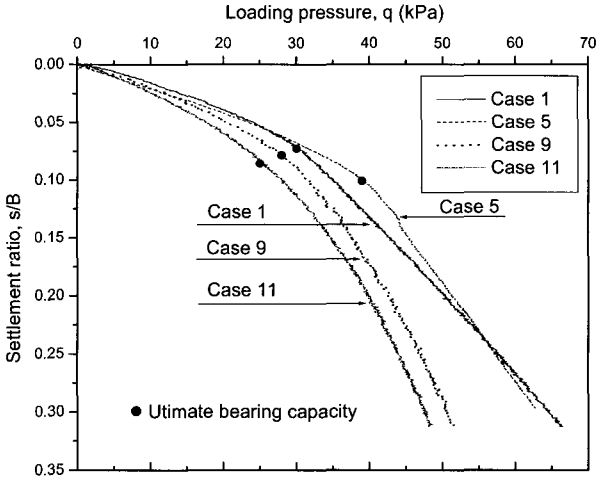

Fig. 17. Bearing capacity-settlement curve in relation to varied location of flexible pipe without reinforcement

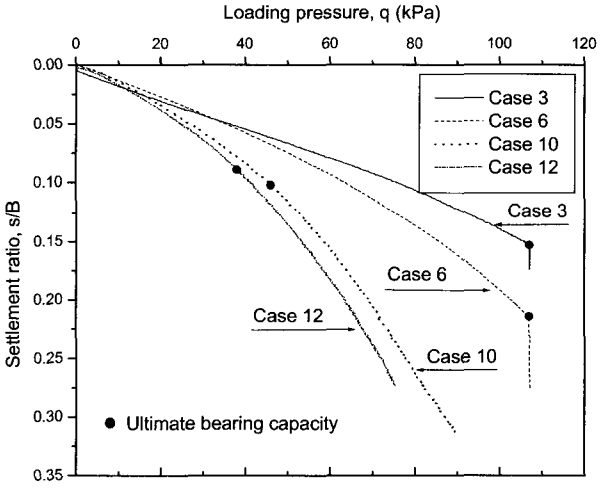

Fig. 18. Bearing capacity-settlement curve in relation to varied location of flexible pipe with reinforcement

the general shapes of the bearing capacity-settlement curve are the same. In Cases 9 and 11 where each flexible pipe is laid 1.9B and 0.6B underneath the foundation, the ultimate bearing capacity and the bearing capacity appear to be lower than in Case 1. The closer the flexible pipe is to the foundation, the less the bearing capacity is: The shape of the bearing capacity-settlement curve also changes from local shear to punching shear.

In Case 3, using reinforced sand, where the only reinforcement is double-layered, and in Case 6, where flexible pipe is laid 1.6B underneath the foundation, their ultimate bearing capacities are shown as equal. However, Case 6 shows an increase of settlement as the bearing capacity increases, and in Cases 10 and 12, where the flexible pipe is laid respectively 1.0B and 0.6B underneath the foundation, the ultimate bearing capacity and the bearing capacity are significantly lower than in Case 3. Moreover, in Cases 3 and 6 the shapes of the bearing capacity-settlement curve show general shear, while Cases 10 and 12 show local shear.

As illustrated in Figs. 17 and 18, when the flexible pipe is laid 1.6B underneath the foundation, the pipe has little effect on the bearing capacity. However, buried depth of the flexible pipe is less than the width of the foundation; the bearing capacity and the ultimate bearing capacity are smaller compared to the no-pipe situation.

Fig. 19 illustrates the bearing capacity-settlement behavior of Cases 1, 11, 12. These tests were conducted to make a comparison between bearing capacity with and without reinforcement. In this figure, the levels of bearing capacity showed Case 12 > Case 1 > Case 11. Even in the case where the flexible pipe is laid 0.6B underneath the foundation, if the reinforcement was double-layered under the foundation, the bearing capacity is greater than in the case without the pipe and reinforcement (Case 1). This shows that the bearing capacity improves significantly when tensile reinforcement is laid underneath a shallow foundation.

Fig. 20 illustrates the bearing capacity ratio with and without reinforcement layers. This is to investigate the reinforcement effect in each case.

This figure shows that the bearing capacity ratio is best when there is no flexible pipe, and as the flexible pipe is laid deeper, the reinforcement effect becomes more favorable. In either case where the flexible pipe is laid at 1.0B and 0.6B from the foundation, the bearing capacity ratio remains almost the same.

Figs. 21 and 22 illustrate the bearing capacity ratio in relation to varied depth of the flexible pipe. The bearing capacity ratio with reinforcement is 1.1~2.5. This indicates that the bearing capacity is more favorable in reinforced sand regardless of the placement depth of the flexible pipe. In unreinforced sand, when the placement depth of the flexible pipe is less than the width of the foundation, the bearing capacity is reduced significantly compared to Case 1. But when the placement depth of

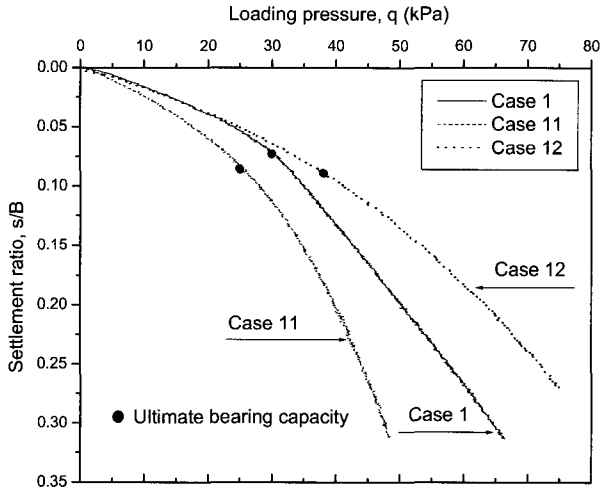

Fig. 19. Comparison of bearing capacity with and without reinforcement

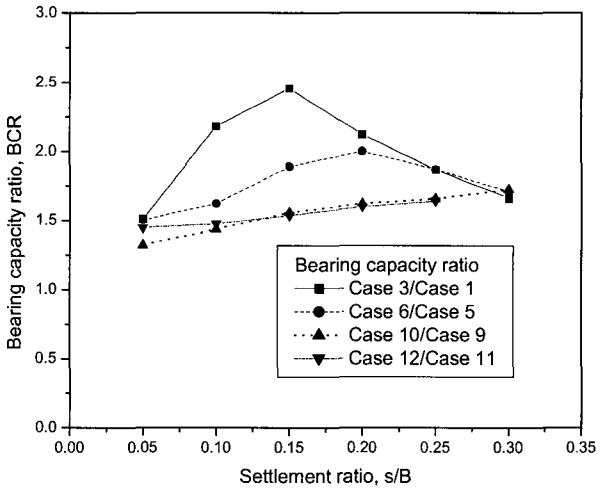

Fig. 20. Influence of varied location of flexible pipe on the reinforcement effect

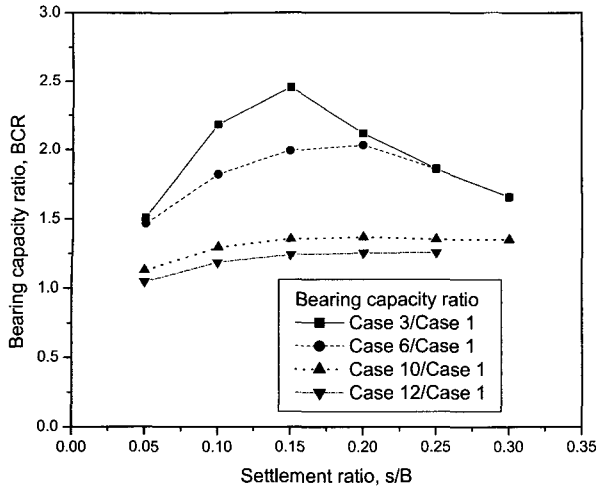

Fig. 21. Bearing capacity ratio in relation to varied depth of flexible pipe with reinforcement

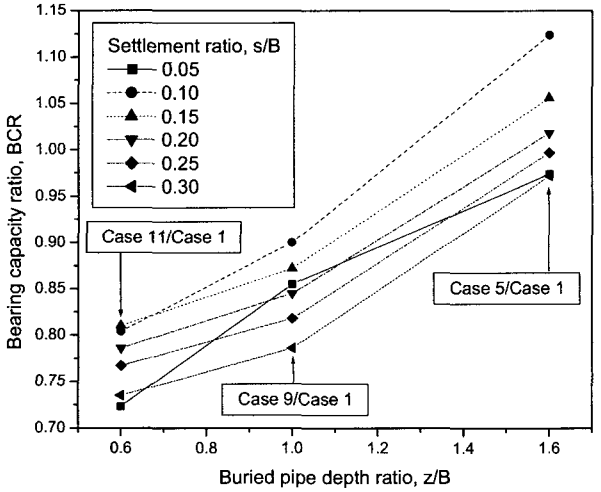

Fig. 22. Bearing capacity ratio in relation to varied depth of flexible pipe without reinforcement

the flexible pipe is 1.6B from the foundation, the bearing capacity ratio is 0.97~1.13, indicating that the placement of the flexible pipe has little effect on the bearing capacity.

5. Conclusion

The main conclusions from the result of this model test are as follows.

Bearing capacity increases significantly with reinforcement in a sand foundation of loose density. The optimal number of reinforcement layers is 2. If more than 2 layers are installed, the bearing capacity decreases slightly compared to the 2 layer situation. In unreinforced sand, the type of failure is local shear, however if more than 2 layers of reinforcement are installed, the type of failure converts from local shear to general shear. At an arbitrary settlement level, the bearing capacity ratio appears to be smaller than the ultimate bearing capacity ratio.

Concerning the improvement of bearing capacity through the use of tensile reinforcement materials, this study has shown that the initial stiffness and shape of the reinforcement are more important than the ultimate tensile strength of the reinforcement.

In the case where a flexible pipe is laid underneath a shallow foundation, when the buried depth of the flexible pipe is 1.6B, the flexible pipe has little effect on the ultimate bearing capacity. However, if the buried depth of the flexible pipe is less than the width of the foundation, the type of failure in reinforced sand changes from general shear to local shear.

Even in the case where a flexible pipe is laid 0.6B underneath a foundation in reinforced sand, the bearing capacity-settlement curve is improved compared to the case without the pipe and reinforcement. This shows that the bearing capacity increases significantly with the installation of reinforcement materials in a loose sand foundation.

Acknowledgements

This study was supported by Columbia University in New York City. The support is gratefully acknowledged.

References

1. Abled-Baki, S., Raymond, G.P. and Johnson, P. (1993), "Improvement of the Bearing Capacity of Footings by A Single Layer of Reinforcement", *Proc., Geosynthetics '93 Conf.*, Canada, pp.407-416.
2. Akinmusuru, J.O. and Akinbolade, J.A. (1981), "Stability of Loaded Footings on Reinforced Soil", *Journal of Geotech Engrg.*, ASCE, Vol.107, No.6, pp.819-827.
3. Binquet, J. and Lee, K.L. (1975a), "Bearing Capacity Tests on Reinforced Earth Slabs", *Journal of Geotechnical Engineering Division*, ASCE, Vol.101, No.12, pp.1241-1255.
4. Binquet, J. and Lee, K.L. (1975b), "Bearing Capacity Analysis of Reinforced Earth Slabs", *Journal of Geotechnical Engineering Division*, ASCE, Vol.101, No.12, pp.1257-1276.

5. Bowles, J.E. (1996), "*Foundation Analysis and Design*", McGraw-Hill Publishing Company, USA, 1175p.
6. Das, B.M., Shin, E.C. and Omar, M.T. (1994), "The Bearing Capacity of Surface Strip Foundations on Geogrid-Reinforced Sand and Clay - A Comparative Study", *Geotechnical and Geological Engineering*, Vol.12, pp.1-14.
7. Fragaszy, R.J. and Lawton, E. (1984), "Bearing Capacity of Reinforced Sand Subgrades", *Journal of Geotechnical Engineering Division*, ASCE, Vol.110, No.10, pp.1500-1507.
8. Guido, V.A., Chang, D.K. and Sweeny, M.A. (1986), "Comparison of Geogrid and Geotextile Reinforced Slabs", *Canadian Geotechnical Journal*, Vol.23, pp.435-440.
9. Guido, V.A., Knueppel, J.D. and Sweeny, A. (1986), "Plate Loading Tests on Geogrid-Reinforced Earth Slabs", *Proc., Geosynthetics '87 Conf.*, New Orleans, pp.216-225.
10. Huang, C.C. and Tatsuoka, F. (1988), "Prediction of Bearing Capacity in Level Sandy Ground Reinforced with Strip Reinforcement", *Proc. Int. Geotech. Symp. Theory and Practice of Earth Reinforcement*, ed. Yamanouchi et al. Balkema, Rotterdam, 1988, pp.191-196.
11. Huang, C.C. and Tatsuoka, F. (1990), "Bearing Capacity of Reinforced Horizontal Sandy Ground", *Geotextile and Geomembranes*, Vol.9, pp.55-82.
12. Khing, K.H., Das, B.M., Puri, V.K., Cook, E.E. and Yen, S.C. (1993), "The Bearing Capacity of A Strip Foundation on Geogrid-Reinforced Sand", *Geotextile and Geomembranes*, Vol.12, pp.351-361.
13. Mandal., J.N. and Manjunath, V.R. (1990), "Bearing Capacity of Single Layer of Geosynthetic Sand Subgrade", *Proceedings of the Indian Geotechnical Conference*, pp.7-10.
14. Omar, M.T., Das, B.M., Puri, V.K. and Yen, S.C. (1993), "Ultimate Bearing Capacity of Shallow Foundations on Sand with Geogrid Reinforcement", *Canadian Geotechnical Journal*, Vol.30, pp.545-549.
15. Samtani, N.C. and Sonpal, R.C. (1989), "Laboratory Tests of Strip Footing on Reinforced Cohesive Soil", *J. Geotech. Engrg.*, ASCE, Vol.115, No.9, pp.1326-1330.
16. Singh, H.R. (1988), "Bearing Capacity of Reinforced Soil Beds", PhD Thesis, Indian Institute of Science, Bangalore, India.
17. Sridharan, A., Murthy, B.R.S., Bindumandhava, F. and Vasudevan, A.K. (1989), "Model Tests on Reinforced Soil Mattress on Soft Soil", *Proc., 12th Int. Conf. on Soil Mech. and Found. Engrg.*, Rio de Janeiro, Brazil, pp.1765-1768.
18. Yetimoglu, T., Wu, J.T.H. and Saglamer, A. (1994), "Bearing Capacity of Rectangular Footings on Geogrid-Reinforced Sand", *Journal of Geotechnical Engineering Division*, ASCE, Vol.120, No.12, pp.2083-2099.

(received on Jul. 5, 2004, accepted on Sep. 23, 2004)